

Crystallization of an Aromatic Biopolyester

Roland Hany,^{*,†} Martin Brinkmann,[‡] Davide Ferri,[§] René Hartmann,[⊥] Ernst Pletscher,[⊥] Daniel Rentsch,[†] and Manfred Zinn[⊥]

[†]Empa, Swiss Federal Laboratories for Materials Testing and Research, Laboratory for Functional Polymers, Überlandstrasse 129, CH-8600 Dübendorf, Switzerland, [‡]Institut Charles Sadron CNRS – Université de Strasbourg, 23 rue du Loess, 67034 Strasbourg, France, [§]Empa, Swiss Federal Laboratories for Materials Testing and Research, Laboratory for Solid State Chemistry and Catalysis, Überlandstrasse 129, CH-8600 Dübendorf, Switzerland, and [⊥]Empa, Swiss Federal Laboratories for Materials Testing and Research, Laboratory for Biomaterials, Lerchenfeldstrasse 5, CH-9014 St. Gallen, Switzerland

Received May 7, 2009; Revised Manuscript Received June 23, 2009

Introduction

Due to their biocompatibility and biodegradability, polyesters from the group of polyhydroxyalkanoates (PHAs) have emerged as promising materials for use in everyday consumer products and various medical and engineering applications.^{1–4} The best-known of these PHAs is poly(3-hydroxybutyrate), PHB, and its copolymer with 3-hydroxyvalerate units, P(HB-co-HV). PHB adopts a 2_1 , left-handed helical conformation in the solid state with an orthorhombic unit cell with $a = 0.576$ nm, $b = 1.32$ nm, and $c = 0.596$ nm (fiber axis).⁵ Recently, temperature-dependent X-ray diffraction and infrared spectra have suggested that hydrogen bondings stabilize the chain folding in the lamellar structure and explain partly the high crystallinities of PHB and PHV.^{6–8}

Medium-chain-length PHAs (mcl-PHAs) containing aliphatic C6–C12 monomeric units have quite different properties with respect to PHB or PHV; they behave like elastomeric thermoplastics of reduced crystallinity (about 25%⁹ vs 60–70%¹⁰) and with lower glass transition ($T_g = -25$ to -40 °C) and melting temperatures ($T_m = 45$ to 60 °C), respectively.¹¹ Similarly to PHB, aliphatic mcl-PHAs crystallize as a 2_1 helix in an orthorhombic lattice with two molecules per unit cell. The structural model involves a succession of sheets with a repeat period of 0.455 nm. Within the sheets, the polymer chains are separated by ~ 1.95 nm because of the extended planar zigzag conformation of the aliphatic side chains.¹² The c axis is significantly shorter (~ 0.45 nm on average) than for PHB; this compression of the helix pitch has been attributed to the effect of the side-chain packing on the overall chain conformation of the PHA backbone.⁹ To our knowledge, the detailed crystal structure of a mcl-PHA has not been reported so far.

For mcl-PHAs containing aromatic side chains, (co-)polymers from 6-phenylhexanoic acid, 7-phenylheptanoic acid, and 8-phenyloctanoic acid (T_g between -14.8 and -1.3 °C) have shown an increase in the glass transition temperature, but are reported to be completely amorphous.¹³ Likewise, for poly(3-hydroxy-5-phenylvalerate), PHPV, the crystallinity has been reported to be very low.^{14,15} Mcl-PHA biosynthesized from 8-(*p*-methylphenoxy)octanoic acid was crystalline ($T_m = 97$ °C),¹⁵ and increased crystallinity and a melting temperature of $T_m = 102$ °C have been reported for a homopolyester containing fluorinated phenoxy side groups.¹⁶

Here, we report on the crystal structure of poly(3-hydroxy-*p*-methylphenylvalerate), PHMePV, which was produced with a

chemostat under well-defined growth conditions.¹⁷ So far, PHMePV has been produced only as a blend with a mcl-PHA from nonanoic acid and in very small amounts.¹⁸ The crystal structure was determined by the combination of transmission electron microscopy (TEM) and molecular modeling using the structure of PHB as a starting point. The PHMePV model reveals short contacts between adjacent polymer chains, indicating that $-\text{CH}_3 \cdots \text{O}=\text{C}$ hydrogen bonding might stabilize the crystal structure. This agrees with results for the related homopolymer PHPV, which was produced similarly and found to be amorphous.

Experimental Section

5-*p*-Methylphenylvaleric acid (MePV) was purchased from Biosynth AG, St. Gallen, Switzerland, 5-phenylvaleric acid (PV) from Fluka. PHMePV and PHPV were produced in a chemostat culture of *Pseudomonas putida* GPO1¹⁹ at a dilution rate of $D = 0.2 \text{ h}^{-1}$ under nitrogen-limited growth conditions.¹⁷ The bacterial culture was fed with a minimal medium²⁰ containing a fixed mixture of lactic acid and PV or MePV respectively (see Supporting Information). The polymers were extracted from freeze-dried cells using methylene chloride and precipitated in methanol as described previously.²¹

The crystallization of PHMePV was performed in propylene carbonate. One drop of a 0.1 wt % solution was deposited between two glass coverslips. The whole was placed in a Linkam hot stage (THMS 600) under nitrogen atmosphere. The solution was heated at 110 °C for one minute to dissolve completely the polymer and cooled at 10 °C min^{-1} to reach the crystallization temperature in the range 20–40 °C. The sample was left for isothermal crystallization during 12–24 h. The formation of crystalline axialites and spherulites was followed with a Leica DMR-X microscope under crossed polarizers or in phase contrast mode. The crystalline domains on the glass substrate were recovered for TEM analysis and were subsequently coated with an amorphous carbon film. The samples were recovered on TEM microscope grids by floating the polymer/carbon films on a diluted HF solution (5 wt %). TEM was performed with a CM12 FEI microscope equipped with a MVIII CCD camera (Soft Imaging Systems, Germany). Molecular modeling was performed on a Silicon Graphic station using the Cerius2 program (Accelrys Ltd. Cambridge, England). An iterative trial-and-error procedure was used to refine the crystal structure of PHMePV (vide infra).

Thermal gravimetric analyses in a helium atmosphere was performed on a TGA7 analyzer from Perkin-Elmer with a heat ramp from 30 to 900 °C at 20 °C min^{-1} ; the weight loss onset was at 308 °C, and the weight residue at 600 °C was 1.4%. Molecular

*To whom correspondence should be addressed. Telephone: +41 44 823 4084. Fax: +41 44 823 4012. E-mail: roland.hany@empa.ch.

weights were measured by gel permeation chromatography (Agilent 1100) in chloroform using a refractive index detector.²² A Perkin-Elmer DSC7 differential calorimeter was used to determine glass and melting temperatures. Samples were heated in a nitrogen atmosphere from -30 to 150 °C at a rate of 20 °C min^{-1} , cooled down to -30 °C at 2 °C min^{-1} , and again heated to 150 °C at 20 °C min^{-1} .

^1H and ^{13}C NMR spectra were recorded at 400.13 (100.61) MHz on a Bruker Avance-400 NMR spectrometer. Experiments in solution were performed at 298 K with standard pulse programs and parameter sets using a 5 mm broadband inverse probe with z-gradient. Diffusion-edited NMR spectra were recorded by applying the flow-compensated double-stimulated-echo experiment (see Supporting Information).²³ Solid-state ^{13}C MAS NMR spectra with ^1H TPPM decoupling were measured at ambient temperature using a 7 mm cross-polarization magic-angle-spinning (CP-MAS) broadband probe with MAS rates of 4800 Hz (only at this spinning frequency all signals of interest did not severely interfere with spinning side bands). Spectra were recorded either as single pulse experiments applying 45° ^{13}C pulses with relaxation delays of 10 or 30 s, or as ^{13}C CP-MAS experiments (see Supporting Information).

Results and Discussion

Biosynthesis. *Pseudomonas putida* GPO1 was continuously cultured in a benchtop bioreactor. The carbon feed was composed of lactic acid as cosubstrate and the PHA substrate was either MePV or PV. This approach using a coffee was found to be a stable way to produce mcl-PHA from inefficient carbon substrates (see Supporting Information). Batch cultures on the aromatic substrates alone did not result in satisfying biomass production due to substrate toxicity (only small concentrations of aromatic substrates could be used) and slow growth rates (only two carbon units per MePV or PV can be used for maintenance energy and growth¹⁴). No polymer was produced with lactic acid alone. PHMePV was a high-molecular weight ($M_w = 147$ kg mol^{-1} , $M_w/M_n = 2.3$) homopolymer (structural purity 97 mol %), and glass and melting temperatures of $T_g = 17 \pm 3$ °C and $T_m = 99 \pm 2$ °C (lit.¹⁸ 17 and 95 °C) were measured. PHPV was produced in an analogous manner. For PHPV, $T_g = 22 \pm 2$ °C (lit.¹⁴ 13 °C; lit.¹⁸ 19 °C) was measured, but no melting endotherm was observed.

Figure 1a shows the ^1H NMR spectrum of PHMePV with the chemical structure and chemical shift assignment. The resonances at ~ 0.9 (1.2) ppm are attributed to $-\text{CH}_3$ ($-\text{CH}_2-$) groups from aliphatic C7–C10 chains with an intensity of approximately 3 mol % compared to PHMePV. Attempts to remove these aliphatic compounds by polymer purification (repeated precipitation in methanol or stirring in acetone or hexane) failed. NMR experiments proved that the aliphatic chains were actually present as polymer side chains that were incorporated during the biosynthesis of PHMePV, probably due to a weak activity of the PhaG enzyme (see Supporting Information). We note that similar observations were made for PHPV (spectra not shown).

Crystallization of PHMePV. PHMePV powder as obtained by precipitating a polymer-chloroform solution in methanol and after filtration and drying was studied with solid-state NMR. ^{13}C MAS NMR spectra show two sets of signals for the carbons at positions C-1 (169.1 and 167.9 ppm) and C-3 (70.6 and 68.5 ppm) (Figure 1c) and for both carbons the resonance at high frequency is broadened (Figure 1d). The relative signal intensities of the narrow resonances generally increased when in the single-pulse experiment the recycle delay between individual pulses was increased from 10 to 30 s and when CP-MAS was performed. Both observations suggest that the component with the narrow signals is more crystalline.^{12,24}

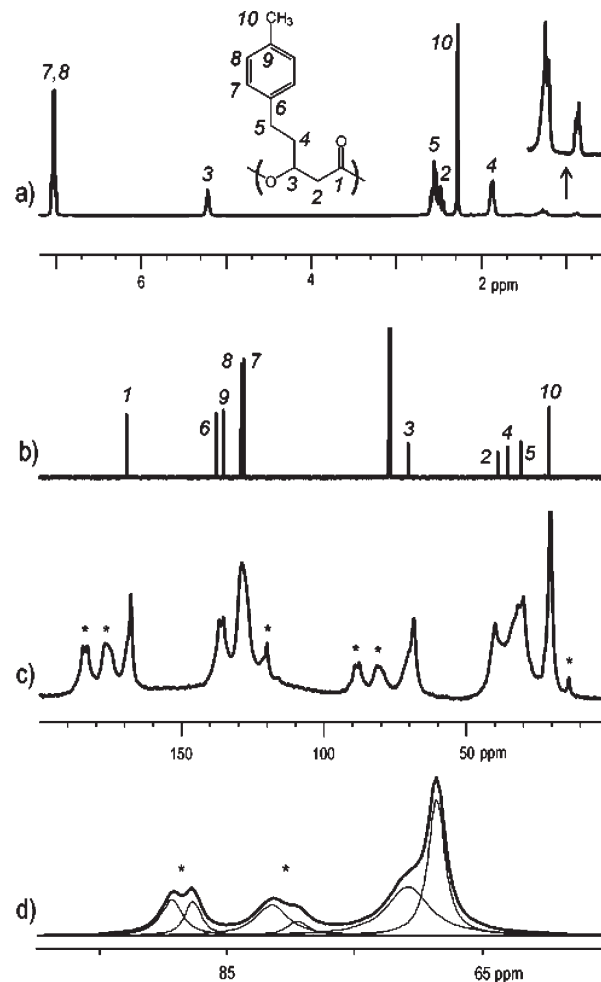


Figure 1. (a) ^1H and (b) ^{13}C NMR spectra of PHMePV in chloroform solution with the polymer structure and signal assignment; solvent signal is at 77.0 ppm in part b. (c) ^{13}C magic angle spinning (MAS) NMR spectra of PHMePV, MAS rate 4.8 kHz, single pulse experiment with recycle delay of 30 s, asterisks denote spinning side bands. (d) Example of line shape analysis performed for C-3 of PHMePV, expansion of full spectrum shown in part c; line widths of 410 and 155 Hz were determined for the amorphous (62%) and crystalline (38%) fractions at 70.6 and 68.5 ppm, respectively; spinning side bands (*) were included in the simulation.

No significant changes of the relative signal intensities between the two components were observed when the contact time of the CP-MAS experiment was varied between 0.2 and 2 ms. Relative fractions were determined by line shape analysis (Figure 1d) using single-pulse Bloch decay MAS experiments that detect both the mobile and more amorphous, as well as the more crystalline and thus rigid components. For both C-1 and C-3 resonances, a crystallinity degree of $40 \pm 2\%$ was determined. The analysis of the ^{13}C CP-MAS spectrum of PHPV exhibited single broad resonances (see Supporting Information). The PHPV resonance of C-3 at 70 ppm had the same line width of 410 Hz as obtained from line shape analysis for the amorphous component in PHMePV (Figure 1d). This supports literature^{14,15,18} and DSC results that the crystallinity of PHPV is very low. In addition, the intensities of the spinning side bands were much smaller than for PHMePV, demonstrating the fast enough motion of the amorphous PHPV to average the chemical shift tensor and dipolar couplings with MAS.¹⁰

The crystallization ability of PHMePV was manifested in different ways depending on the crystallization conditions, leading either to banded spherulites or branched multilamellar

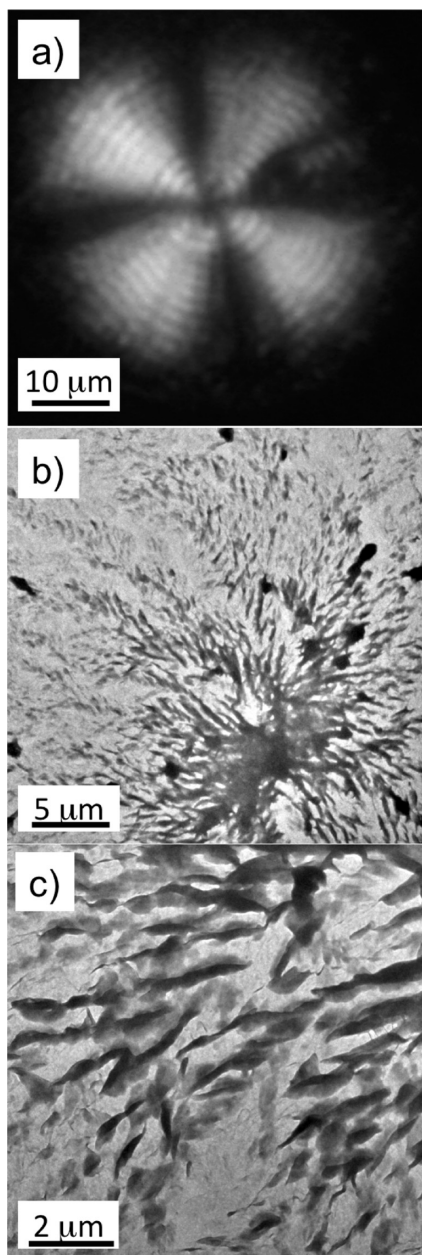


Figure 2. (a) Banded spherulite of PHMePV observed with a polarized optical microscope. The spherulites were formed via solvent-induced crystallization by exposing an amorphous thin film of PHMePV to vapors of acetone. (b) TEM bright field image showing the branched lamellar structure of PHMePV obtained by slow crystallization of a diluted (0.1 wt %) solution in propylene carbonate at 40 °C. (c) Enlarged view showing the typical lamellar twisting.

structures or axialites. As seen in Figure 2a, banded spherulites of PHMePV with a band periodicity of $\sim 1 \mu\text{m}$ were obtained upon exposure of an amorphous cast film to acetone vapor. The spherulites present the typical Maltese cross and concentric extinction bands under the polarized optical microscope. The banded structure of the spherulites is due to the regular twisting, causing a helical torsion of the crystalline lamellae.²⁵ In the case of PHB, the twisting axis was shown to coincide with the *a* axis of the unit cell.²⁶ In banded spherulites of PHV, both left- and right-handed lamellar twisting has been evidenced recently.²⁷

A different morphology was obtained when the polymer was isothermally crystallized from a solution in propylene carbonate. Highly branched multilamellar structures were

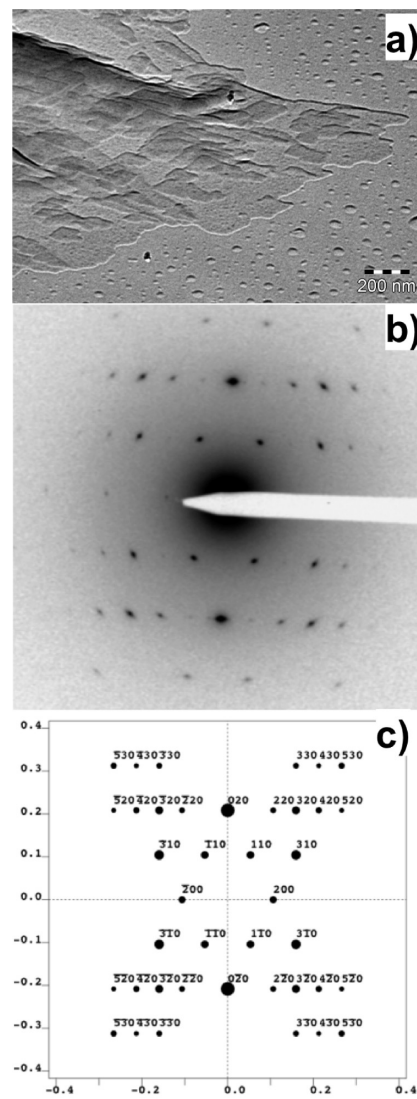


Figure 3. (a) TEM bright field image showing a multilamellar crystal of PHMePV. Note the presence of daughter lamellae on top of the mother lamella. (b) Electron diffraction (ED) pattern in proper relative orientation to the bright field image. (c) Calculated ED pattern using the refined crystal structure of PHMePV with proper indexing of the reflections.

observed by optical microscopy in phase contrast and by TEM (Figures 2b,c) when PHMePV was crystallized at 40 °C. Investigation of the lamellar structures by TEM evidence a typical twisting of single lamellae with a regular pitch when radiating out from the core to the periphery of the axialite. This twisted axialite-like morphology is reminiscent of the banded spherulite structure of PHMePV observed in acetone vapor exposed films. In polyethylene, it was proposed that the twisting of the lamellae is due to unbalanced stresses on the opposite surfaces of the lamellae.²⁸ More specifically, in the case of chiral polymers, Lotz and Cheng²⁹ proposed that the stress originates from different chain conformations on the two opposite sides of the lamellae. Similar experiments were performed in order to crystallize PHPV. However, the crystallization conditions used for PHMePV did not allow us to crystallize PHPV.

Crystal Structure Determination. In order to study the crystal structure of PHMePV, we used selected area electron diffraction to obtain a detailed electron diffraction pattern as seen in Figure 3b. This diffraction pattern suggests

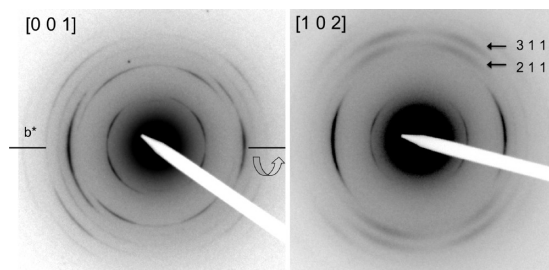


Figure 4. Electron diffraction patterns of an oriented PHMePV sample. The ED pattern on the right was obtained upon rotation of the sample $\pm 55^\circ$ around the b^* axis.

orthorhombic symmetry as observed for PHV. Characteristic extinctions of certain reflections, e.g. $([2n+1] 0 0)$ and $(0 [2n+1] 0)$, n is an integer, are observed, suggesting the presence of two 2_1 screw axes along the a and b axes of the unit cell. Accordingly, the two-dimensional space group can be defined as p_{2gg} and the cell parameters are $a = 0.96 \pm 0.05$ nm, $b = 1.88 \pm 0.05$ nm, and $\gamma = 90^\circ$. It is worth noting that the value of the a parameter compares well with that observed in PHV⁵ ($a = 0.95$ nm), whereas the b parameter is much larger (b of PHV = 1.01 nm), reflecting the presence of the methyl-phenyl side groups (vide infra).

In order to determine the full unit cell for PHMePV, we resorted to a rotation-tilt experiment that allows the indirect determination of the c parameter. Upon rotating an oriented area of the sample around the b^* axis, we observed a characteristic pattern depicted in Figure 4 at an angle $\theta = 55^\circ$. This pattern shows two typical reflections which can be indexed consistently as $(2 1 1)$ and $(3 1 1)$ assuming that the c parameter amounts to 0.57 ± 0.04 nm. In addition, this value is consistent with the observed tilt angle of 55° (vs calculated angle of 59°). The extracted c value is very close to that reported for PHB and PHV ($c = 0.596$ and 0.556 nm, respectively).^{5,6,30}

PHAs are isotactic and the chiral center at the 3-position is in the R -configuration. For PHB and PHV, the chains adopt a left-handed helix. The fiber repeat reflects the tacticity of the chain, i.e. for a syndiotactic chain involving alternating R and S centers a fiber repeat of approximately 0.769 nm is expected vs 0.596 nm for an isotactic chain of PHB.⁸ The fact that the c parameter of PHMePV is close to that of R-PHB and R-PHV strongly suggests that PHMePV is essentially isotactic and shows the R configuration, which is furthermore expected from the biosynthetic route. The isotactic character of the chains of PHV and PHB is manifested in the corresponding crystal structures by the presence of a 2_1 screw axis parallel to the c axis. We therefore suggest that the space group of PHMePV is also $P2_12_12_1$, as for PHB and PHV. In order to obtain a meaningful density of the crystal, the unit cell must contain two chains and four monomer repeat units in proper symmetry relation. With this unit cell content, the calculated crystal density yields a consistent value of 1.23 g cm⁻³ (1.25 g cm⁻³ for PHB⁸).

Modeling of the Crystal Structure. As the starting point of the structural model of PHMePV, we used the backbone of PHB on which we have "grafted" the methyl-phenyl side groups of PHMePV. The structure of the PHB backbone used hereafter has been proposed by Brückner et al. and is based on a Rietveld refinement.³¹ The first step of the structural modeling was to determine the appropriate azimuthal orientation of the PHMePV chain in the a, b plane of the unit cell. The best orientation corresponds to the situation where the methyl-phenyl side groups point in the direction parallel to the b axis of the unit cell. The second step

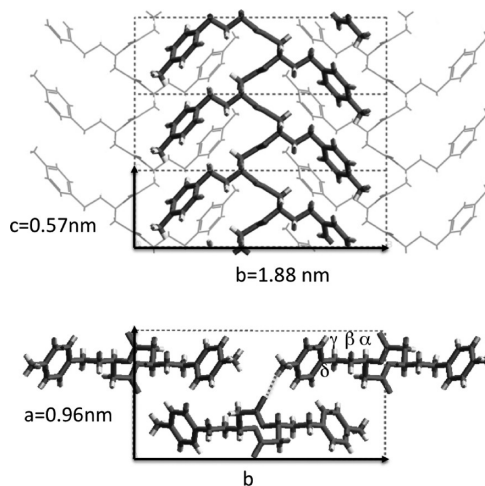


Figure 5. Projection of the refined structure of PHMePV along the c and the a axis. The structure is tentatively characterized by an orthorhombic cell with $P2_12_12_1$ symmetry and cell parameters $a = (0.96 \pm 0.05)$ nm, $b = (1.88 \pm 0.05)$ nm, $c = (0.57 \pm 0.04)$ nm, and $\alpha = \beta = \gamma = 90^\circ$. For the $[001]$ projection, an interchain short contact that may correspond to a $C=O \cdots H-C$ hydrogen bond is highlighted.

consisted in determining the most likely orientation of the methyl-phenyl side groups on the PHV backbone. To this aim, we have used a trial-and-error method. This method consists in (i) determining the positions of the chains in the unit cell and (ii) determining the most probable side chain conformation. For the determination of the latter, we have rotated sequentially the methyl-phenyl side group around the $C_\alpha-C_\beta$, $C_\beta-C_\gamma$ and the $C_\gamma-C_\delta$ bonds (Figure 5) to obtain the best match between the calculated and the experimental ED patterns of the $[0 0 1]$ zone (Figures 3b,c). The calculated ED pattern is in very good agreement with the experimental pattern although little discrepancies concerning the intensity ratio between 110 and 310 reflections are observed. In particular, the strongest reflections corresponding to $0 2 0$, $1 1 0$, $3 1 0$, and $3 2 0$ reflections are reproduced with proper relative intensities. Also noteworthy is the absence of the $1 2 0$ reflection in both calculated and experimental ED patterns. Figure 5 shows the projections of the tentative structure projected along the chain axis (c axis) and along the a axis.

As for PHB and PHV, the crystal structure involves two antiparallel chains with left-handed conformation packed in an orthorhombic unit cell. With respect to PHV and PHB, the main difference in the chain packing stems from the presence of the methyl-phenyl side groups. In the structural model proposed herein, we observe that the methyl-phenyl side groups are oriented on either side of the backbone along the b axis. The distance between the methyl end groups on either side of the backbone, projected on the b axis is found to match perfectly the length of the b axis. Of interest is the presence of short contacts between adjacent polymer chains. Significant short contacts are found between the oxygen atom of the carbonyl group of one chain and the hydrogen atom of the methyl group of the adjacent chain. The refined structural model depicted in Figure 5 indicates that these $C-H \cdots O=C$ contacts have a length of 0.24 – 0.26 nm. Such short contact may correspond to $C-H \cdots O=C$ hydrogen bonds as has been evidenced recently in the case of PHB and PHV.^{6,7} In the latter systems, hydrogen bonding are reported to play an important role in the peculiar chain folding leading to stable lamella structure and high crystallinity. We propose that similar arguments apply to PHMePV and that hydrogen bonding between the $-CH_3$ group of one

chain and the O=C group of another chain stabilize the crystal structure; this then also might explain the very low tendency of PHPV to crystallize, where the corresponding $-\text{CH}_3$ group is not present. Initial results from temperature-dependent infrared spectra support this view (see Supporting Information).

Conclusion

In this work, we report the crystal structure determination of a mcl-PHA made of 3-hydroxy-*p*-methylphenylvalerate repeating units. Both mcl-PHAs and short-chain-length PHAs such as PHB and PHV are isotactic which should provide for an ordered packing in the solid state. Still, mcl-PHAs are generally of lower crystallinity compared to PHB or PHV. One reason for this is that, due to bacterial physiology, most mcl-PHAs are random copolymers and consist of two or more polymer repeating units, which hinders a regular chain arrangement. As has been shown for aliphatic mcl-PHAs, the side chain and backbone carbon undergo also very different dynamics, and the relatively fast-moving hydrocarbon side chains act as a diluent which hinders the crystallization.^{9,10} Given these arguments, the higher crystallinity of PHMePV appears plausible, because it is essentially a homopolymer and the dynamics of the bulky phenyl side chain is probably slower than that of a straight carbon chain of equal length. The same arguments, however, do not explain the very low crystallization tendency of the corresponding homopolymer PHPV, since also phenylpropionate is no substrate for growth or PHA formation,¹⁴ and the polymer side chain is of comparable size. We suspect that $-\text{CH}_2\text{H}\cdots\text{O}=\text{C}$ hydrogen bonds stabilize the structure and partly explain the higher crystallinity of PHMePV.

Acknowledgment. We thank T. Geiger (Empa) for GPC, E. Fischer (Empa) for TGA, and C. Walder (Empa) for DSC measurements.

Supporting Information Available: Text giving details of the biosynthesis and NMR analysis, such as results of variable temperature IR experiments on PHMePV and PHPV, a scheme showing the structure of PHMePV, and figures showing NMR, and IR spectra. This material is available free of charge via the Internet at <http://pubs.acs.org>.

References and Notes

- (1) Steinbüchel, A.; Valentin, H. E. *FEMS Microbiol. Lett.* **1995**, *128*, 219.
- (2) Sudesh, K.; Abe, H.; Doi, Y. *Prog. Polym. Sci.* **2000**, *25*, 1503.
- (3) Hazer, B.; Steinbüchel, A. *Appl. Microbiol. Biotechnol.* **2007**, *74*, 1.

- (4) Chen, G.-Q.; Wu, Q. *Biomaterials* **2005**, *26*, 6565.
- (5) Marchessault, R. H.; Yu, G. In *Biopolymers*; Doi, Y., Steinbüchel, A., Eds.; Wiley-VCH: Weinheim, Germany, 2002; Vol. 3b, pp 157–203.
- (6) Sato, H.; Ando, Y.; Dybal, J.; Iwata, T.; Noda, I.; Ozaki, Y. *Macromolecules* **2008**, *41*, 4305.
- (7) Sato, H.; Mori, K.; Murakami, R.; Ando, Y.; Takahashi, I.; Zhang, J.; Terauchi, H.; Hirose, F.; Senda, K.; Tashiro, K.; Noda, I.; Ozaki, Y. *Macromolecules* **2006**, *39*, 1525.
- (8) Doi, Y. *Microbial Polyesters*, VCH Publishers, Inc.: Weinheim, Germany, 1990.
- (9) Marchessault, R. H.; Monasterios, C. J.; Morin, F. G.; Sundararajan, P. R. *Int. J. Biol. Macromol.* **1990**, *12*, 158.
- (10) Morin, F. G.; Marchessault, R. H. *Macromolecules* **1992**, *25*, 576.
- (11) Preusting, H.; Nijenhuis, A.; Witholt, B. *Macromolecules* **1990**, *23*, 4220.
- (12) Dufresne, A.; Reche, L.; Marchessault, R. H.; Lacroix, M. *Int. J. Biol. Macromol.* **2001**, *29*, 73.
- (13) Abraham, G. A.; Gallardo, A.; Roman, J. S.; Olivera, E. R.; Jodra, R.; García, B.; Miñambres, B.; García, J. L.; Luengo, J. M. *Biomacromolecules* **2001**, *2*, 562.
- (14) Fritzsche, K.; Lenz, R. W.; Fuller, R. C. *Makromol. Chem.* **1990**, *191*, 1957.
- (15) Kim, Y. B.; Kim, D. Y.; Rhee, Y. H. *Macromolecules* **1999**, *32*, 6058.
- (16) Takagi, Y.; Yasuda, R.; Maehara, A.; Yamane, T. *Eur. Polym. J.* **2004**, *40*, 1551.
- (17) Zinn, M.; Witholt, B.; Egli, T. *J. Biotechnol.* **2004**, *113*, 263.
- (18) Curley, J. M.; Hazer, B.; Lenz, R. W.; Fuller, R. C. *Macromolecules* **1996**, *29*, 1762.
- (19) van Beilen, J. B.; Panke, S.; Lucchini, S.; Franchini, A. G.; Röthlisberger, M.; Witholt, B. *Microbiology* **2001**, *147*, 1621.
- (20) Hartmann, R.; Hany, R.; Geiger, T.; Egli, T.; Witholt, B.; Zinn, M. *Macromolecules* **2004**, *37*, 6780.
- (21) Zinn, M.; Weilenmann, H.-U.; Hany, R.; Schmid, M.; Egli, T. *Acta Biotechnol.* **2003**, *23*, 309.
- (22) Hany, R.; Böhlen, C.; Geiger, T.; Hartmann, R.; Kawada, J.; Schmid, M.; Zinn, M.; Marchessault, R. H. *Macromolecules* **2004**, *37*, 385.
- (23) Jerschwo, A.; Müller, N. *J. Magn. Reson.* **1997**, *125*, 372.
- (24) Spyros, A.; Marchessault, R. H. *J. Polym. Sci., B: Polym. Phys.* **1996**, *34*, 1777.
- (25) Xu, J.; Guo, B.-H.; Zhang, Z.-M.; Zhou, J.-J.; Jiang, Y.; Yan, S.; Li, L.; Wu, Q.; Chen, G.-Q.; Schultz, J. M. *Macromolecules* **2004**, *37*, 4118.
- (26) Gazzano, M.; Focarete, M. L.; Riekel, C.; Ripamonti, A.; Scandola, M. *Macromol. Chem. Phys.* **2001**, *202*, 1405.
- (27) Ye, H.-M.; Xu, J.; Guo, B.-H.; Iwata, T. *Macromolecules* **2009**, *42*, 694.
- (28) Keith, H. D.; Padden, F. J., Jr. *Polymer* **1984**, *25*, 28.
- (29) Lotz, B.; Cheng, S. Z. D. *Polymer* **2005**, *46*, 577.
- (30) Iwata, T.; Doi, Y. *Macromolecules* **2000**, *33*, 5559.
- (31) Brückner, S.; Meille, S. V.; Malpezzi, L.; Cesàro, A.; Navarini, L.; Tombolini, R. *Macromolecules* **1988**, *21*, 967.